Effect of fabrication parameters on the vibro-acoustic behavior of 3-D printed membrane-type resonators

Uğur Dinçer[1], Carlos Bothor, Erik Johannsen, Malte Misol, Hans Peter Monner
Institute of Lightweight Systems, German Aerospace Center (DLR e.V.)
Lilienthalplatz 7, 38108 Braunschweig, Germany

ABSTRACT

The rising interest in acoustic metamaterial applications stems from the ability to manipulate sound waves through locally resonant structures. Membrane-type resonators continue to arouse the curiosity of researchers, particularly because of their potential for low-frequency sound insulation purposes. When designing a membrane-type resonator, the magnitude of stress within the membrane is a critical factor in attenuating targeted frequencies. The fused deposition modeling (FDM) method offers versatile fabrication options for resonator design via multi-material printing capabilities. The residual stress resulting from the one-shot printing process of a thin, flexible membrane and a relatively rigid frame is expected to vary according to the fabrication parameters. To address this, the effect of these parameters within the FDM process on the pre-stress of membrane resonators is examined. This study involves modal analysis to determine pre-stress using a laser Doppler vibrometer, with results compared to numerical simulations. Finally, the sound transmission loss of selected samples is measured using an impedance tube.

1. INTRODUCTION

Membranes play a crucial role in sensing and transduction applications, offering selective recognition, signal amplification, and functional adaptability. They are extensively employed across diverse fields, including their use as transducers in microphones and micro-scale acoustic sensing devices integrated within microelectromechanical systems (MEMS) [1]. Additionally, membranes are utilized in aerospace applications as structural components in antennas, and are also employed in musical instruments, such as drumheads [2, 3]. Apart from their conventional applications, the increasing demand for low-frequency sound attenuation using lightweight materials has led to the development of novel structures known as membrane-type acoustic metamaterials (M-AMMs) [3–5]. In M-AMMs, the sound attenuation property of a unit cell is primarily determined by two main components: the mass attached to the membrane and the membrane's pre-stress. Adjusting one or both of these parameters enables tunability to achieve the desired vibro-acoustic response [4, 5]. Although the effects of mass have been extensively studied in the literature, the membrane pre-stress has generally been examined from a numerical perspective for M-AMMs. The main reason for this focus on numerical methods is that measuring and controlling the membrane pre-stress remains a

[1]Ugur.Dincer@dlr.de

significant experimental challenge. Nevertheless, accurately determining the magnitude of pre-stress is crucial for achieving effective sound attenuation [4].

Additive manufacturing enables unrestricted design capability and constructs functional structures by depositing material layer-by-layer [6, 7]. A previous study has demonstrated that multi-material printing using the fused deposition modeling (FDM) technique offers a reliable and repeatable approach for fabricating membrane-type acoustic metamaterial unit cells [5]. In the multi-material printing process, a flexible filament is first used to fabricate the membrane. Then, within the same process, a relatively rigid filament is deposited to form the frame directly on top of the membrane. In this way, the unit cell is fabricated in a one-shot printing process [5].

Due to the differing coefficients of thermal expansion (CTEs) of polymer materials, differential shrinkage occurs during the multi-material printing process. This mismatch results in residual thermal stresses within the final structure [6, 8]. These residual thermal stresses are the main source of pre-stress in the membrane structure. In addition, fabrication parameters such as print speed, cooling rate, and layer height determine the thermal gradients and solidification rates within the printed parts [6, 8]. Similarly, variations in these parameters can affect heat distribution and bonding strength, contributing to non-uniform shrinkage, which often results in internal stresses. Therefore, it is essential to investigate how fabrication parameters influence the induced pre-stress, particularly in relation to the membrane's vibro-acoustic behavior.

The dynamic analysis of membrane structures is typically conducted using non-destructive testing methods to evaluate their mechanical properties. One such approach is vibro-acoustic testing, which utilizes a sound source to excite the membrane and measure its frequency response. The measured frequency response is subsequently used to derive the mechanical properties of the membrane. This approach enables accurate determination of the pre-stress within the membrane [1, 2, 9]. Furthermore, the experimental data obtained from the dynamic analysis of the samples provide a reliable basis for creating a numerical model of the M-AMMs. Therefore, finite element analysis software can be used to integrate experimentally obtained data into the numerical model and to numerically investigate the effect of pre-stress on the modal behavior of the samples [10]. This enables direct comparison with the experimental results. The sound insulation properties of the M-AMMs can be accurately evaluated using the two-load method with four microphones in an impedance tube. This technique enables measurement of the sound transmission loss behavior of the samples, providing an assessment of their acoustic performance [4, 5].

In this study, the effects of printing parameters on the vibro-acoustic behavior of 3D-printed membrane-type resonators are investigated. Section 2 describes the fabrication of unit cell samples using a multi-material printing approach with both flexible and rigid filaments. To examine the influence of printing parameters, variations are introduced in the membrane's printing pattern, as well as in the layer height and printing speed of the supporting frame. This section also defines the method used to determine the pre-stress in the membrane and presents a corresponding numerical model developed to analyze its modal behavior. Subsequently, selected samples are experimentally evaluated using an impedance tube to assess their sound transmission loss (STL) characteristics, with a focus on applications in membrane-type acoustic metamaterials. Section 3 discusses the results obtained from experimental measurements and numerical simulations. Finally, Section 4 presents the conclusions and outlook for future research.

2. FABRICATION AND CHARACTERIZATION OF SAMPLES

2.1. Design and Printing of Resonators

In order to investigate the vibro-acoustic behavior of the structure, a representative unit cell must first be designed to reflect the fundamental characteristics of a membrane-type resonator. Since the analytical model and the mechanical behavior of circular membranes are well established, the unit cell is designed accordingly and is illustrated in Figure 1. Besides, the physical dimensions of the sample used throughout the study are provided in Table 1.

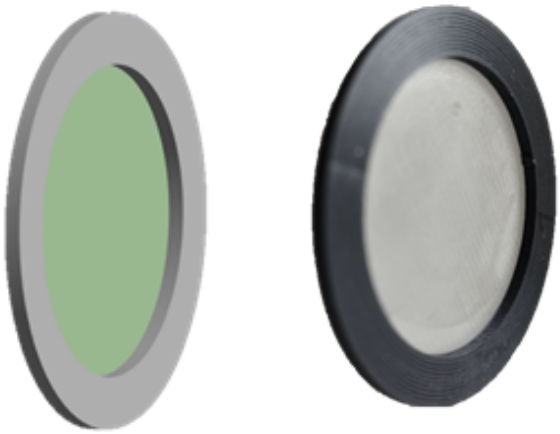

(a) 3-D model of sample. (b) Fabricated sample.

Figure 1: Designed and fabricated unit cell sample.

The previous work has demonstrated the compatibility of thermoplastic polyurethane (TPU) and polyethylene terephthalate glycol (PETG) for multi-material printing using the fused deposition modeling (FDM) technique in a one-shot printing process [5]. In this research, the membrane part is fabricated using Ninjaflex 85A [11], while the frame is printed with Prusament PETG [12]. All specimens are fabricated using an Original Prusa MK4S fused deposition modeling (FDM) 3D printer.

Table 1: Physical dimensions of designed sample.

Parameter	**Dimension (mm)**
Unit Cell Diameter	40
Frame Inner Diameter	30
Frame Thickness	1.5
Membrane Thickness	0.1

Through the research, the layer height, the printing speed, and the printing pattern are identified as fundamental parameters influencing thermal expansion and mechanical properties in additive manufacturing, as reported in the literature [7, 8]. Therefore, the samples are printed using different parameter settings, as presented in Table 2. The membrane part of the unit cell is printed in the initial two layers using a flexible filament (TPU) with a layer thickness of 0.05 mm. Moreover, the printing speed is kept constant at 20 mm/s to prevent potential failures associated with poor layer quality. For all samples, the frame printing pattern is maintained as concentric to ensure continuous nozzle movement during fabrication. Once the resonator printing is completed, the samples are left on the print bed until the bed temperature drops to 30°C to prevent deformation or damage during removal.

Table 2: Unit cell fabrication parameters.

Sample Code	Membrane	Frame	
	Printing Pattern	Layer Height (mm)	Printing Speed (mm/s)
Unit Cell_1	Rectilinear	0.05	30
Unit Cell_2	Concentric	0.05	30
Unit Cell_3	Aligned Rectilinear	0.05	30
Unit Cell_4	Rectilinear	0.1	30
Unit Cell_5	Rectilinear	0.2	30
Unit Cell_6	Rectilinear	0.05	50
Unit Cell_7	Rectilinear	0.05	70
Unit Cell_8	Rectilinear	0.2	70
Unit Cell_9	Rectilinear	0.2	140

2.2. Experimental Measurement

The pre-stress resulting from the multi-material printing process is expected to vary across samples and is measurable via experimental modal analysis. The first resonance frequency is obtained from a non-parametric system identification, which involves exciting the membrane with a sound source and measuring the surface displacements as a function of frequency using a laser Doppler vibrometer (LDV). This resonance frequency is then used to calculate the pre-stress in the membrane [1–3, 9]. In this way, the pre-stress in the unit cells can be investigated and compared. For this purpose, the experimental setup shown in Figure 2 is implemented. The setup consists of a loudspeaker that excites the samples using a pseudo-random sound wave in the frequency range of 0–1000 Hz, a Polytec PSV-400 3D scanning laser Doppler vibrometer (LDV) to measure the resulting surface displacements, and an amplifier to drive the sound source. The frequency response is then measured at 61 scan points and analyzed using Polytec software, which processes the measured data to extract the frequency response characteristics of the samples.

During non-parametric system identification, the samples are under fixed boundary conditions while mounted on the sample holder. Therefore, the pre-stress is calculated using the equation below [1]:

$$f_{0,1} = \frac{J_{0,1}}{\pi D} \times \sqrt{\frac{\sigma_0}{\rho}} \tag{1}$$

In Equation 1, $f_{0,1}$ represents the measured first resonance frequency (for the fundamental mode (0,1)), while ρ is the membrane density, with the diameter D under the stress σ_0 . The constant $J_{0,1}$ refers to the first zero of the Bessel function for the first nodal circle (0,1) that has a value of 2.40 [1].

2.3. Finite Element Analysis

In this study, modal analysis is conducted using ANSYS Mechanical Workbench. The unit cell is modeled using the material properties of PETG [12] and TPU [11] filaments provided by the manufacturers, as listed in Table 3.

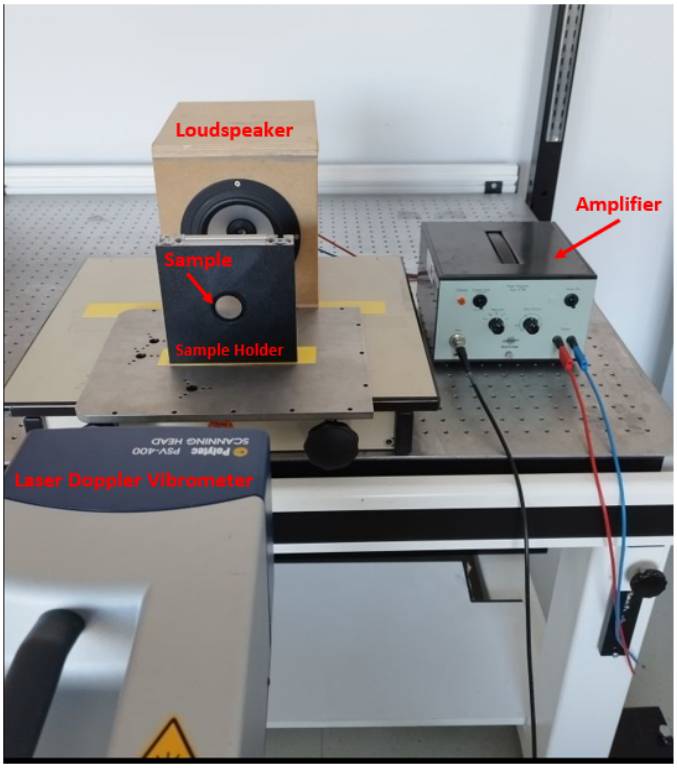

Figure 2: Experimental setup.

Table 3: Material properties of filaments.

Property	**PETG**	**TPU**
Density (kg/m^3)	1270	1190
Tensile Strength, Yield (MPa)	46	4
Tensile Modulus (MPa)	1500	12
Poisson's Ratio	0.35	0.45

The first step is to define the pre-stress measured from the experiments to the membrane part of the model. This is implemented using an ANSYS Programmable Design Language (APDL) command called INISTATE, as detailed in the previous research [10]. Afterwards, the mode shapes and corresponding frequencies obtained from the measurements are compared with those predicted by the finite element model to evaluate its accuracy and reliability.

2.4. Sound Transmission Loss Measurement

In addition to frequency response measurements and finite element analysis, the sound attenuation properties of the selected samples are analyzed. For this purpose, a standard 100 mm diameter impedance tube (AcoustiTube®) is used. The samples are tightly placed into the impedance tube using a sample holder, and the sound transmission loss is measured using the standard Two-Load Method. The acquired data are then processed using AED 1401 measurement software.

3. RESULTS AND DISCUSSION

To evaluate the repeatability of both the sample fabrication process and the measurement methodology, five Unit Cell_1 samples are fabricated in sequential 3D printing processes and characterized using the setup illustrated in Figure 2. Displacement-based frequency response

functions are acquired using the Polytec acquisition software. Figure 3a illustrates the frequency response curves obtained from five Unit Cell_1 samples, indexed as 1 to 5. Distinct and sharp resonance peaks are observed consistently around 200 Hz, indicating the first resonance frequency ($f_{0,1}$) of each sample [1]. These frequencies are subsequently used to calculate the corresponding pre-stress values, as described by Equation 1. For clarity, both the first resonance frequencies and the derived pre-stress values are summarized in Figure 3b. The left vertical axis displays the measured resonance frequencies (black markers) in Hz, while the right vertical axis indicates the calculated pre-stress values (red markers) in MPa. The sample names are shown along the horizontal axis. Based on the first resonance frequencies, the calculated pre-stress values for the Unit Cell_1 samples are approximately 0.07 MPa, with minor variations attributed to fabrication tolerances and measurement uncertainty.

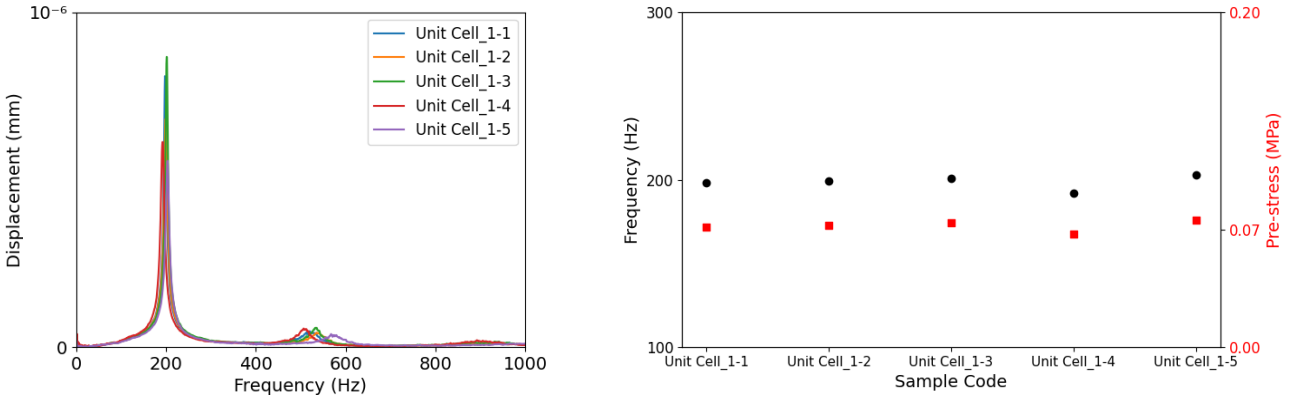

(a) LDV measurement curves.

(b) The first resonance frequencies and pre-stress values.

Figure 3: Investigation of repeatability of the measurement approach.

As reported in the literature [7], the printing pattern is considered a critical process parameter due to its significant influence on the mechanical behavior of the final structure. Furthermore, the coefficient of thermal expansion (CTE) of 3D-printed structures is known to be anisotropic, varying with the printing direction and the pattern [13]. For this purpose, the membrane parts of Unit Cell_2 and Unit Cell_3 are fabricated with concentric and aligned rectilinear infill strategies, respectively. Therefore, the frequency responses and the corresponding pre-stress values of the samples are presented in Figure 4. A slight decrease in the first resonance frequency is observed in Unit Cell_2 compared to Unit Cell_1. This shift can be attributed to the use of a circular bead deposition pattern in Unit Cell_2, which results in reduced heat transfer between adjacent beads compared to the linear pattern used in Unit Cell_1. The weak heat transfer between the beads from the edge toward the center results in lower residual thermal forces, thereby reducing the pre-stress within the membrane. In contrast, when the membrane is printed using an aligned rectilinear pattern, as in Unit Cell_3, a slight increase in the first resonance frequency is observed. This behavior is consistent with a higher level of pre-stress induced by the more efficient heat transfer and associated thermal forces. Although a change in the frequency response is observed, it is still in the repeatability range mentioned above. Consequently, further investigation is required to conclusively determine the influence of the printing pattern on the membrane pre-stress.

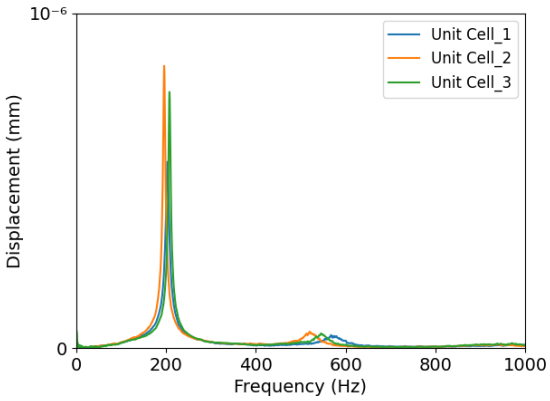

(a) LDV measurement curves.

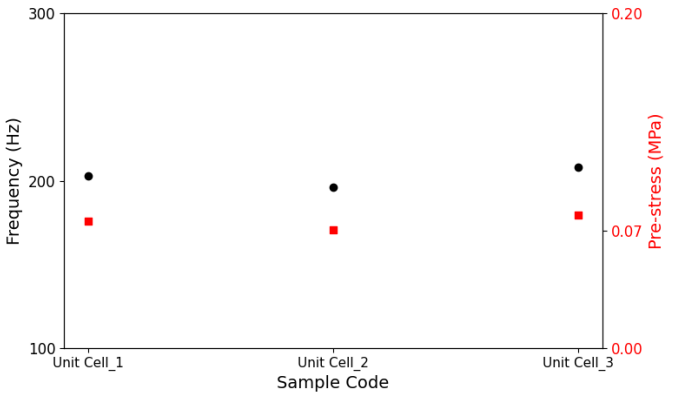

(b) The first resonance frequencies and pre-stress values.

Figure 4: Investigation of membrane printing pattern on the pre-stress of the unit cells.

To investigate the effect of layer height on the pre-stress of the membrane, the frames of Unit Cell_4 and Unit Cell_5 are fabricated using layer heights of 0.1 mm and 0.2 mm, respectively. The frequency response and the corresponding pre-stress values are presented in Figure 5. Increasing the layer height used for frame fabrication results in a shift of the first resonance frequency to approximately 250 Hz. This corresponds to an increase in the pre-stress of over 50%, rising from 0.07 MPa to 0.11 MPa. However, increasing the layer height from 0.1 mm to 0.2 mm does not result in a noticeable change in the pre-stress values, i.e., the frequency response. It can be considered that raising the layer height increases the thermal gradients due to slower cooling, which, when combined with CTE mismatches in multi-material prints, leads to greater residual stress.

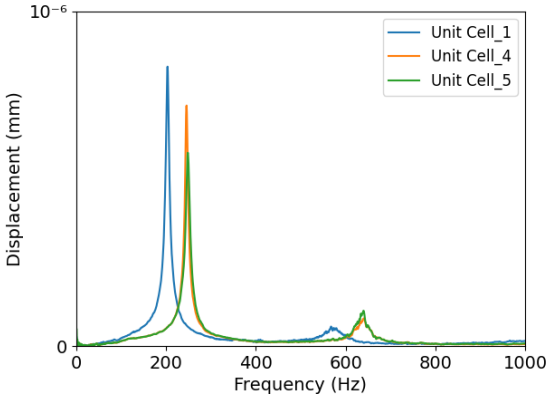

(a) LDV measurement curves.

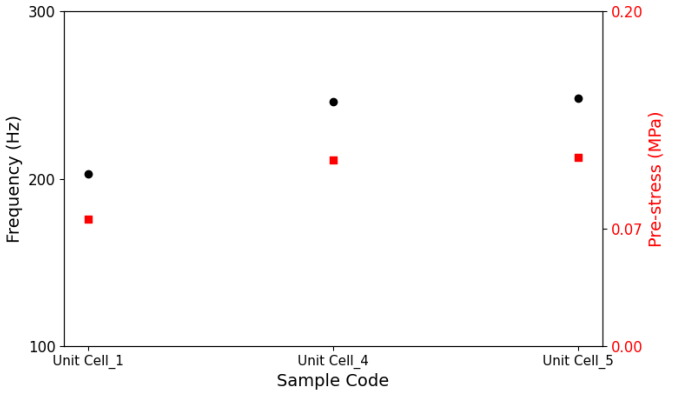

(b) The first resonance frequencies and pre-stress values.

Figure 5: Investigation of layer height on the pre-stress of the unit cells.

The effect of the printing speed of the frame on the membrane's pre-stress is investigated by fabricating Unit Cell_6 and Unit Cell_7 at printing speeds of 50 mm/s and 70 mm/s, respectively, while keeping the layer height constant at 0.05 mm. The results for the frequency response and the corresponding pre-stress values are presented in Figure 6. Increasing the printing speed from 30 mm/s to 50 mm/s results in a shift of the first resonance frequency to 265 Hz, corresponding to an increase in the pre-stress of over 80%, reaching 0.13 MPa for Unit Cell_6. Similarly, for Unit Cell_7, increasing the speed to 70 mm/s further shifts the first resonance frequency to 278 Hz, corresponding to a pre-stress value of 0.14 MPa. This can be attributed to the reduced cooling time between layers, which leads to higher thermal gradients and insufficient stress relaxation during solidification.

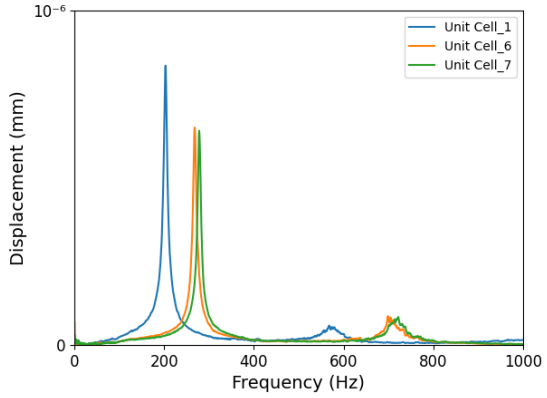

(a) LDV measurement curves.

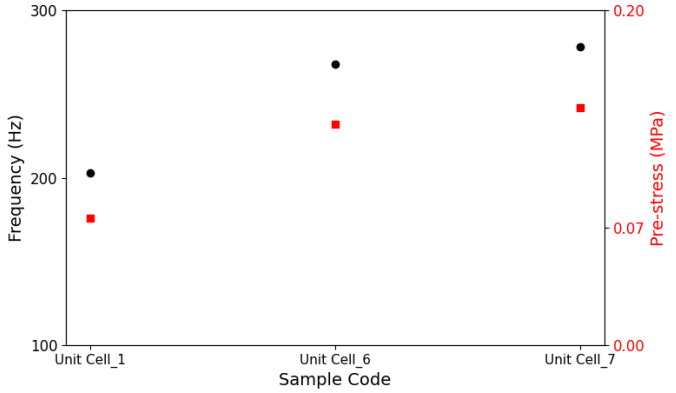

(b) The first resonance frequencies and pre-stress values.

Figure 6: Investigation of printing speed on the pre-stress of the unit cells.

To further investigate the effect of printing speed on the membrane pre-stress, the samples Unit Cell_8 and Unit Cell_9 are fabricated using a layer height of 0.2 mm and printing speeds of 70 mm/s and 140 mm/s, respectively. The results are compared with those of Unit Cell_5, which is printed using the same layer height but at a printing speed of 50 mm/s, as presented in Figure 7. As already shown in Figure 6, increasing the printing speed of the frame also increases the pre-stress in the membrane when using a layer height of 0.2 mm. The pre-stress values of Unit Cell_8 and Unit Cell_9 show an increase of over 15% relative to Unit Cell_5.

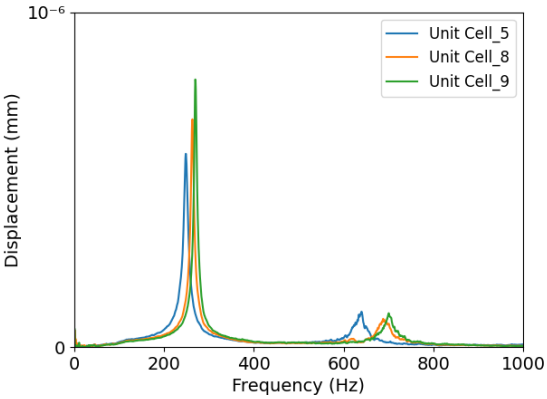

(a) LDV measurement curves.

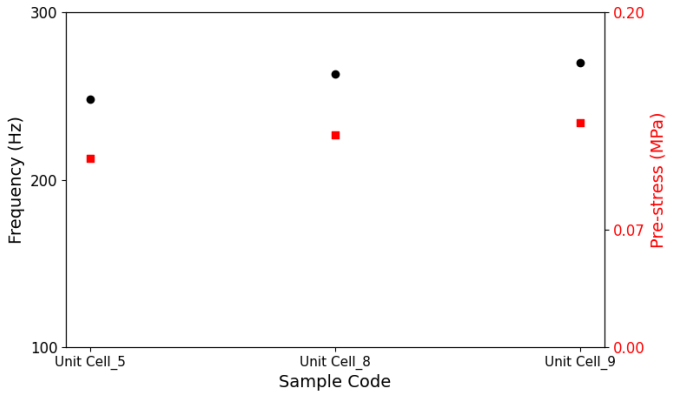

(b) The first resonance frequencies and pre-stress values.

Figure 7: Investigation of printing speed on the pre-stress of the unit cells for 0.2 mm layer height.

The pre-stress values derived from experimental measurements of the first resonance frequencies are applied to the membrane part of the equivalent model in ANSYS Mechanical Workbench. Furthermore, a fixed boundary condition is applied to the top surface of the frame, consistent with the setup used in the experimental measurements. Afterwards, modal analysis is implemented via the Modal module in Mechanical Workbench. Figure 8 presents the frequencies obtained for the selected samples through both experimental measurements and finite element analysis, along with the corresponding mode shapes for the respective mode numbers. For the first mode (0,1) of the samples, a perfect match is observed between the experimental results and the finite element analysis. However, for the (1,1) mode, a deviation of approximately 6% is observed between the experimental results and the finite element analysis. Similarly, for the (0,2) mode, this deviation is determined to be around 12%. These discrepancies for higher modes are likely due to

the inability to replicate the experimental conditions as precisely as in the simulation, the modeling approach of the material, and the neglect of damping in the model as reported in the literature [2].

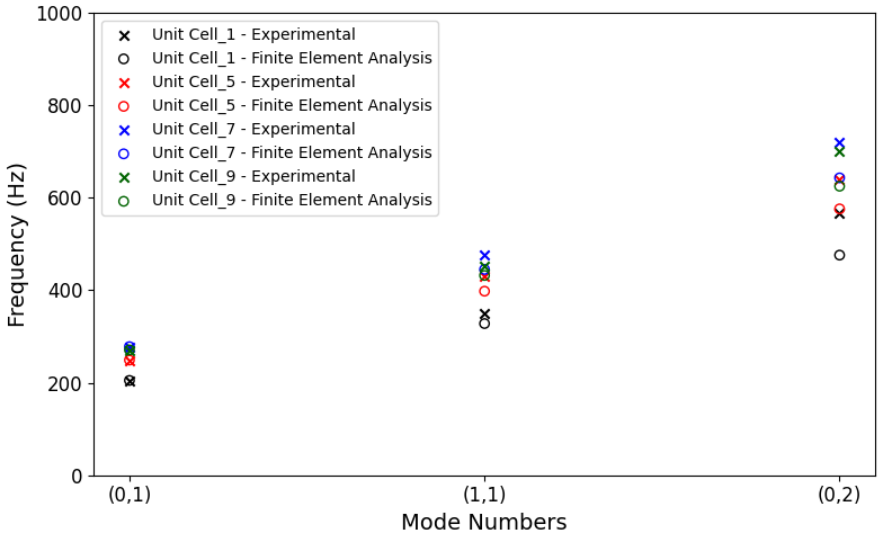

(a) Frequencies for corresponding mode numbers.

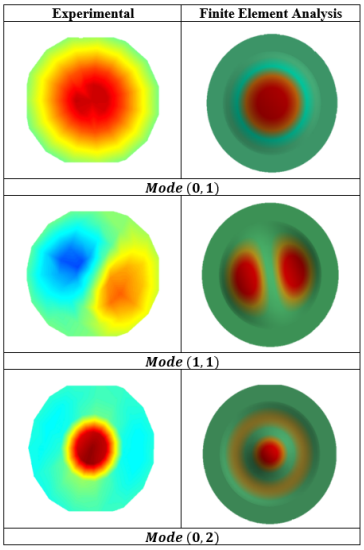

(b) Mode shapes for corresponding mode numbers.

Figure 8: Comparison of experimental and finite element analysis results of selected samples.

The sound insulation properties of the fabricated samples, intended for potential membrane-type acoustic metamaterial applications, are investigated using an impedance tube. The results for the selected unit cells are presented in Figure 9. The first dip observed between 200–250 Hz in the sound transmission loss curves corresponds to the first resonance frequency, the mode (0,1), of the samples. At this frequency, the structure vibrates with maximum amplitude, resulting in peak sound transmission [4, 10]. For a circular membrane, the mode (1,1) is not symmetric and involves motion in opposite phases. Therefore, since an acoustic plane wave applies uniform pressure, this mode is not excited, and its effect is not observed in sound transmission loss measurements [4]. The behavior observed between 500–700 Hz corresponds to the mode (0,2) of the unit cell samples. In this mode, out-of-phase motion between the regions inside and outside the second nodal circle creates an acoustic short-circuit effect, leading to a peak in transmission loss [4, 10]. As previously demonstrated in the earlier figures, increasing the pre-stress shifts the frequency response toward higher values. A similar trend is also observed in the sound transmission loss behavior of the samples.

4. CONCLUSION AND OUTLOOK

In this study, the effects of printing parameters on membrane-type resonator structures are investigated for their potential application in acoustic metamaterials. To achieve this, the samples are fabricated using a multi-material 3D printing approach, in which the membrane's printing pattern and the frame's printing height and speed are varied in a one-shot process. The frequency responses of the unit cells are measured using a laser Doppler vibrometer (LDV) under excitation from a sound source. The resulting frequency response curves are then used to estimate and compare the pre-stress values in the membranes. Initially, five identical samples are fabricated to evaluate the repeatability of the manufacturing and measurement processes. After confirming consistency, the printing parameters are varied and examined. Among the parameters studied, the printing speed showed the most significant effect, while the membrane's layer height and printing pattern had a comparatively minor influence. Increasing the frame's printing speed led to higher membrane pre-stress, which in turn shifted the frequency response to higher frequencies. Additionally, finite element models (FEM) of selected samples are developed, implementing the pre-stress values

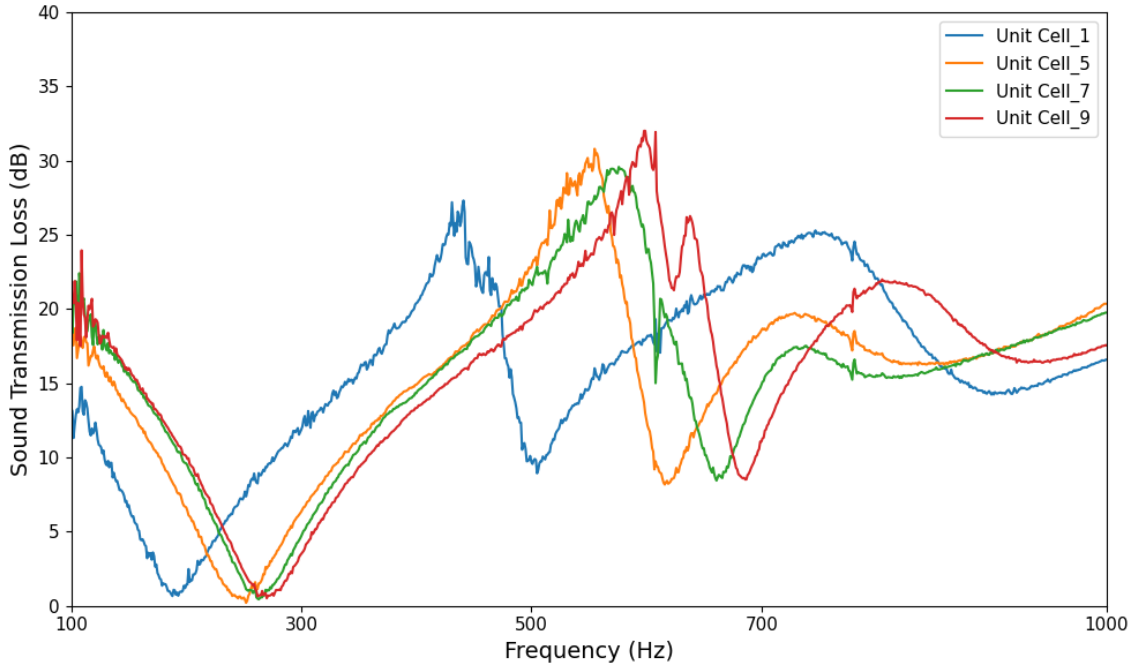

Figure 9: Sound transmission loss of selected unit cells.

obtained from experimental data. A strong correlation is observed in the first resonance mode between the experimental and FEM results. However, discrepancies became more remarkable in higher-order modes, likely due to experimental imperfections not accounted for in the simulations. To further investigate the sound insulation properties of the samples, sound transmission loss (STL) measurements are conducted using an impedance tube. Similar behavior is observed between the LDV-based frequency response and the STL results for the first resonance frequency of the selected samples. Overall, the findings demonstrate that modifying the printing parameters can effectively alter membrane pre-stress, enabling tunable vibro-acoustic behavior in acoustic metamaterials. This approach offers a promising strategy for tailoring metamaterials to target specific frequency ranges for sound attenuation applications. Future work may focus on investigating the effects of additional process parameters, such as cooling time, fan speed, and extrusion factor, while incorporating thermal measurements to gain deeper insights and support the estimation of residual thermal forces.

ACKNOWLEDGEMENTS

This study was realized using the facilities of the German Aerospace Center (DLR) - Braunschweig and supported by the Republic of Turkey Ministry of National Education.

REFERENCES

1. R. I. Haque, E. Ogam, P. Benaben, and X. Boddaert. Inkjet-Printed Membrane for a Capacitive Acoustic Sensor: Development and Characterization Using Laser Vibrometer. *Sensors*, 17(5):1056, 2017.
2. M. Kamper and A. Bekker. Non-contact experimental methods to characterise the response of a hyper-elastic membrane. *International Journal of Mechanical and Materials Engineering*, 12(12), 2017.
3. C. Casarini, V. Romero-García, J.-P. Groby, B. Tiller, J. F. C. Windmill, and J. C. Jackson. Fabrication and Characterization of 3D Printed Thin Plates for Acoustic Metamaterials Applications. *IEEE Sensors Journal*, 19(22):10365–10372, 2019.

4. F. Ma, C. Wang, C. Liu, and J. Wu. Structural designs, principles, and applications of thin-walled membrane and plate-type acoustic/elastic metamaterials. *Journal of Applied Physics*, 129(23):231103, 2021.
5. U. Dinçer, M. Misol, and H. P. Monner. Characterization of Membrane-Type Acoustic Metamaterial Unit Cells Fabricated by Additive Manufacturing Methods. In *10th Convention of the European Acoustics Association, EAA 2023*, September 2023.
6. A. Nazir, O. Gokcekaya, K. M. M. Billah, O. Ertugrul, J. Jiang, J. Sun, and S. Hussain. Multi-material additive manufacturing: A systematic review of design, properties, applications, challenges, and 3D printing of materials and cellular metamaterials. *Materials Design*, 226:111661, 2023.
7. Rowin J. M. Bol and Branko Šavija. Micromechanical Models for FDM 3D-Printed Polymers: A Review. *Polymers*, 15(23):4497, 2023.
8. L. R. Lopes, A. F. Silva, and O. S. Carneiro. Multi-material 3D printing: The relevance of materials affinity on the boundary interface performance. *Additive Manufacturing*, 23:45–52, 2018.
9. A. Lima-Rodriguez, J. Garcia-Manrique, W. Dong, and A. Gonzalez-Herrera. A Novel Methodology to Obtain the Mechanical Properties of Membranes by Means of Dynamic Tests. *Membranes*, 12(3):288, 2022.
10. U. Dinçer, S. Algermissen, M. Misol, and H. P. Monner. Modeling of 3-D printed membrane-type acoustic metamaterial unit cells and investigating the dynamic behaviors. In *Active and Passive Smart Structures and Integrated Systems XVIII*, volume 12946, page 129460O, 2024.
11. NinjaTek. Ninjaflex materials data sheet. https://ninjatek.com/shop/ninjaflex/. Last accessed 2024-12-15.
12. Prusament. Petg materials data sheet. https://prusament.com/de/materials/prusament-petg/. Last accessed 2024-12-15.
13. E. Johannsen and H. P. Monner. Manufacturing of Mono-Material Tunable Thermal Expansion Structures using Additive Extrusion. In *SAMPE Europe Conference Exhibition 2024, 24-26.09.2024, Belfast*, 2024.